Vision Research 216 (2024) 108363

Contents lists available at ScienceDirect

Vision Research

journal homepage: www.elsevier.com/locate/visres

Motion-induced blindness as a noisy excitable system

Mikhail Katkov [*], Alexander Cooperman [1], Noya Meital-Kfir, Dov Sagi

Department of Brain Sciences, The Weizmann Institute of Science, Rehovot, Israel

ARTICLE INFO

Keywords:
Stochastic resonance
Phase locked response
Disappearance inducers
Periodic stimulation

ABSTRACT

Perceptual disappearance of a salient target induced by a moving texture mask (MIB: Motion-Induced Blindness) is a striking effect, currently poorly understood. Here, we investigated whether the dynamics of MIB qualify as an excitable system. Excitable systems exhibit fast switches from one state to another (e.g., visible/invisible) induced by an above-threshold perturbation and stimulus-independent dynamics, followed by a refractory period. In the experiments, disappearance was induced by masks consisting of slowly rotating radial bars with a gap at the target location, leading to periodic perturbation of the visual field around the target (a bright parafoveal spot). When passed around the target location, masks frequently induced an abrupt target disappearance, pointing to locality. As expected from excitable systems, the disappearance time was not affected by additional bars crossing the target during invisibility, and there was little dependence on the mask configuration. After the target reappeared, it stayed for at least 0.5–2 s (the refractory period). Therefore, the dynamics governing MIB represent an example of an excitable system, where the transition to the invisible state is induced by the mask. The dynamics that follow were determined mostly by the internal network properties.

1. Introduction

Motion-Induced Blindness (MIB) is a striking phenomenon where a moving mask suppresses the perception of a physically present static target (Bonneh, Cooperman, & Sagi, 2001). MIB disappearances are an all-or-none phenomenon and can last up to several seconds, even with a high-contrast target located near fixation (Bonneh, Donner, Cooperman, Heeger, & Sagi, 2014). Furthermore, invisibility can be perturbed by a similar visible cue flashed at the target neighborhood (Meital-Kfir & Sagi, 2018), indicating that the neuronal networks involved in invisibility preserve sensitivity. Despite the detailed experimental exploration of MIB, the underlying mechanism remains unknown. Here, we considered applying the theory of dynamical systems, which was found to be useful in describing bistable phenomena.

MIB, with the corresponding spontaneous transition between seen and not-seen states, is often treated as a bistable phenomenon (Bonneh et al., 2014; Devyatko, Appelbaum, & Mitroff, 2017; Hsu, Yeh, & Kramer, 2006; Jaworska & Lages, 2014). MIB was found to be affected by stimulation parameters in a way similar to that of binocular rivalry; the two phenomena show a highly correlated pattern of perceptual transitions across individuals (Carter & Pettigrew, 2003). Others point to the large individual differences in MIB measurements as a modeling challenge, arguing that "normative models of MIB may not be practical" (Sparrow, LaBarre, & Merrill, 2017).

One interesting approach to describe bistable phenomena involves modeling a stable percept as an attractor state, which can be defined as the persistent activity of a group of neurons (Braun & Mattia, 2010; Cao, Pastukhov, Aleshin, Mattia, & Braun, 2021). In this model, the irregular switching between percepts is governed by intrinsic noise, which drives the network state between the two attractors. The mechanism underlying switching can be described as follows: there is a basin of attraction around attractor states, meaning that in the absence of noise, the system would return to the attractor state when perturbed, making switching impossible. However, the presence of noise introduces random perturbations that can move the system outside of the current basin of attraction into the basin of another attractor.

When an external periodic perturbation or signal is introduced, an intriguing phenomenon can occur. The external signal effectively alters the relative sizes of the basins of attraction for the two attractor states. A smaller basin of attraction increases the probability of escaping it. When

* Corresponding author.
E-mail address: mikhail.katkov@gmail.com (M. Katkov).

[1] This article is dedicated to the memory of Dr. Alexander Cooperman (1930-2019) for his tremendous contribution and initiative. Alex Cooperman first envisioned the possibility of describing MIB as a dynamical system; he carried out many pilot studies but did not have enough time to complete his work. An earlier version of this work was presented at the 2015 meeting of the Israeli Society for Neuroscience.

https://doi.org/10.1016/j.visres.2024.108363
Received 12 January 2023; Received in revised form 28 December 2023; Accepted 17 January 2024

the size change is significant, there is a marked difference in switching probability during the different phases of the signal. The level of noise plays a crucial role in determining the system's behavior. For instance, a small amount of noise introduces weak perturbations, resulting in a low probability of switching during all signal phases. Conversely, in the presence of high levels of noise, the system dynamics are predominately governed by noise, leading to a similar switching behavior across all the phases. However, with intermediate noise levels, the switching probability varies substantially across the different signal phases. Here, switching predominantly occurs during the favorable phase of the signal. This phenomenon, characterized by an increased frequency component in the switching behavior, a frequency corresponding to the stimulus frequency, is known as stochastic resonance (see the Supplementary Material for an illustration).

An important difference between MIB and other bistable phenomena, such as binocular rivalry, lies in the number of stable states. Whereas in bistable phenomena two percepts may equally last for prolonged periods, in MIB the invisibility state is unstable, exhibiting a transient behavior. In dynamical systems theory, such behavior characterizes excitable systems. For example, consider a spiking neuron. In the absence of a strong input, the neuron is in a resting state – small input fluctuations lead to small fluctuations in the membrane potential, tracking the input frequency. However, when the input exceeds the threshold level, the neuron responds with a large-scale excursion in phase space (action potential). Once an action potential is initiated, the membrane potential changes substantially and is weakly dependent on the input. The temporal profile of the spike largely depends on the properties of the neuron, but not on the properties of the input. When the action potential ends, there is a measurable refractory period during which the neuron cannot emit spikes.

In a manner similar to a bistable system, excitable systems can also exhibit stochastic resonance. In the absence of noise or external perturbation, the dynamics of a bistable system converge to one of the stable states, whereas in an excitable system would converge to its resting state. In the presence of a sufficient amount of noise, a bistable system switches between stable states, whereas an excitable system repeatedly undergoes a large excursion; each trajectory ends at its resting state. The detailed dynamics underlying these transitions, which depend on the strength of the noise and the properties of the system, can be explored using periodic external stimulation. A stimulation period that is close to the characteristic system time constant is expected to facilitate switching at a stimulation frequency. In contrast, when the stimulation frequency is too high, the system, while in transit toward its stable state, is insensitive to external stimulation and is not expected to be affected by the frequent incoming stimulation. When the stimulation frequency is too low, since intrinsic dynamics is faster than the driving frequency, several switches are possible during a single stimulation period that broadens the response in the frequency domain. Overall, this looks like a noise-assisted resonance – there is a specific noise-dependent frequency of stimulation that leads to optimal switching (Longtin & Chialvo, 1998; Muratov, Vanden-Eijnden, & Weinan, 2005; Volkov, Ullner, Zaikin, & Kurths, 2003; Gammaitoni et al., 1998).

Bistable models assume that perception corresponds to the proximity of the dynamical system state to one of the attractors. However, when considering perception in an excitable system, this assumption needs to be clarified. Regarding motion-induced blindness (MIB), the perceptual disappearance of a target does not align with any specific attractor state. We can draw a parallel to memory retrieval in an attractor neural network, where retrieval occurs when the system approaches one of its attractor states associated with a memory. Similarly, in MIB, when the system diverges sufficiently from the attractor state representing the target and there are no attractor states near the system trajectory, the target perceptually disappears. Under this interpretation, within the limit of low noise, we can anticipate several characteristics: (1) excitation of the system leads to a long excursion, determined by the system dynamics, followed by relaxation to a visible resting state. This excursion results in a substantial, non-zero duration of invisibility; (2) there is a refractory period, which represents the minimal visibility time required before the target can disappear again; and (3) the signal-to-noise ratio (defined as the switching amplitude at stimulus frequency relative to other frequencies, see the Methods section) exhibits a non-monotonic dependency on the mask frequency. Regarding high noise levels, we still expect a substantial mean visibility period, and the dependence of the signal-to-noise ratio on the mask frequency may be less pronounced or even disappear together with the refractory period.

In our study, we employed two types of stimulation to investigate motion-induced blindness (MIB):

1. Static Mask: We used a fixed mask that did not change over time or an absent mask, which resulted in perceiving the Troxler effect. The Troxler effect (Troxler, 1804) refers to the perceptual disappearance of a static target when it is presented away from the viewer's fixation point.
2. Periodic Stimulation: We employed periodic stimulation to study the dynamics of MIB while considering the mask as a driving force. This allowed us to explore how the presence of a moving mask influences the perceptual switches in MIB.

Although perceptual fluctuations in the presence of static and periodic masks were found to be affected differently by the stimulation parameters, some similarities were noted (Bonneh et al., 2014). The experiments with a static mask allowed us to define a switching baseline of a resting state, shared by the two stimulation types. We found that the frequency of the disappearance events in the static mask condition varied continuously 5-fold across observers. In our experiments, observers displaying a small frequency of disappearance events in the static condition exhibited the behavior expected from excitable systems, whereas observers having a large frequency of disappearances in the static condition showed smaller effects. This suggests that a significant portion of the switches observed in the latter group were not directly related to the presence of the moving mask. Observers that had many disappearance events in the static mask condition also had short invisibility periods, whereas observers with few invisibility periods in the static mask condition had longer invisibility periods, rarely shorter than 400 ms, indicating the presence of a minimum duration of invisibility in MIB conditions (similar to the findings by Meital-Kfir et al., 2016). Furthermore, for most participants, regardless of the mask condition, the visible periods were not shorter than 1–2 s, indicating the presence of a refractory period. Our results indicate that a non-monotonic relationship exists between the SNR and the stimulation frequency. This suggests that the switching behavior in MIB is influenced by the frequency of the applied stimulation.

2. Methods

2.1. Human observers

This study was approved by the Weizmann Institute of Science Ethics Committee and the Helsinki Committee. Ten human observers with normal or corrected-to-normal vision participated in the experiment. Before the experimentation, all observers provided their informed consent under the approved Declaration of Helsinki.

Six observers with normal or corrected-to-normal vision participated in all experiments.

2.2. Stimuli

This study included 6 experimental conditions. Stimuli consisted of a static target (yellow dot, 0.5 deg in diameter) placed at 6 deg in the upper-left visual field and a fixation point (a white dot 0.25 deg in diameter). These elements were present in all conditions. In the Troxler condition, no additional elements were present on the screen. In the

other 5 conditions, there was either a static or a rotating mask. The mask consisted of lines placed along six rays originating near the fixation point and form a 60° angle between each pair of rays. Each ray was composed of two distinguishable lines to avoid local interactions with the target during mask rotation. A similar "protection zone" was also maintained between the mask and the fixation point. The inner line started at 1.25 deg of visual angle and ended at 4.6 deg, whereas the outer line started at 7 deg and ended at 10.5 deg. In the rotating mask conditions, the rays were rotated clockwise with constant angular velocity. The angular velocity was chosen so that the periods of motion (i.e., the time between identical images on the screen) were 1, 2, 4, or 8 sec.

2.3. Procedure

After signing a consent form, the observers performed several daily sessions (minimum 6, maximum-12). In each daily session, the observers performed three blocks of trials, 20 minutes each. A mandatory 15-minute break separated the blocks. Each trial was self-initiated by the observer and lasted 120 sec. During the trial, the observers were instructed to fixate on a central fixation point and report when the target is perceptually invisible by pressing and holding the space bar on a computer keyboard until the target becomes visible.

2.4. Empirical characteristic function

The characteristic function is formally defined as.

$$\varphi_X(\omega) = E\left[e^{i\omega X}\right]$$

where E[.] is the expected value, and $i = \sqrt{-1}$ and X are random variables. Empirical distribution functions were computed by substituting samples from X,

$$\varphi_X(\omega) = \sum_{k=1}^{n} e^{i\omega x_k}$$

where X_k is the k-th data point out of n. Absolute values of $\varphi_X(\omega)$ are shown on graphs. $\varphi_X(0) = 1$ by definition, and if X has a periodic density function, there is only one non-zero value of $\varphi_X(\omega)$ corresponding to the period of density function.

2.5. Fitting procedure

We fitted the disappearance distributions as the sum of two random variables: one having a Weibull distribution and the other having a Gamma distribution.

$$\begin{aligned} X &= X_1 + X_2 \\ X_1 &\sim \frac{1}{\sigma\sqrt{2\pi}} x^{a-1} e^{-\frac{x}{b}} \\ X_2 &= \frac{b}{a}\left(\frac{x}{a}\right)^{b-1} e^{-\left(\frac{x}{a}\right)^b}, x \geqslant 0 \end{aligned} \tag{1}$$

The Gamma distribution was previously used to fit bistable phenomena (Carter & Pettigrew, 2003; Devyatko et al., 2017). Additionally, we assumed that there is a minimal delay required for the deterministic trajectory to return to a stable fixed point when the system is excited, and that some jitter exists in the motor responses, which we attempted to capture by the Weibull distribution. We used many tuples of samples (10^6 for each set of parameters) where the first elements of a tuple consisted of samples from the Gamma distribution, and the second element of a tuple consisted of samples from the Weibull distribution. The values of tuples were added to have a sample from the theoretical distribution, which in turn, were used to form an empirical cumulative distribution, and finally, the intermediate values of the theoretical cumulative distribution function (CDF) were estimated by linear interpolation. Using interpolated CDF, we estimated the p-value of the Kolmogorov–Smirnoff goodness of fit. The obtained p-values were used as a cost function in an optimization procedure that consisted of 2 consecutive runs of Genetic Algorithm (GA (Deb, 1999), as implemented in the Matlab ® optimization toolbox). Repeating this procedure with the best value found in the first round as seed values for a second round of GA increased the chances of finding better solutions. However, this method does not guarantee that no good fit to the data exists when our procedure failed to find one.

2.6. Signal-to-noise ratio analysis

To compute the Signal-to-Noise Ratio (SNR), we created a signal representing the perceptual states as a function of time. The visible target was assigned the value '1' and the invisible target was assigned the value '0' discretized at 1 ms precision. All trials were concatenated, sequentially forming a single signal for every observer. SNR was defined as the ratio between the peak amplitude at a stimulation frequency within a narrow band (~2–10 mHz) of an expected stimulation frequency and an average amplitude in a wider frequency window ($16\frac{2}{3}$ times wider). More specifically, a Fast Fourier Transform was computed on the generated signal and a narrow band was selected as 5 frequency bins around the expected frequency, whereas the wide band contained 100 frequency bins. An illustration is provided in Fig. 7

3. Results

To efficiently track the dependence of perceptual transitions on a mask structure, we employed masks consisting of discrete, well-defined parts. The mask (Fig. 1) consisted of bars rotating around a fixation point (with breaks inserted to avoid physical interference with the target); the number of bars and their speed was varied to control the mask angular frequency (see the Methods section). The important timescale is the time interval between consecutive events where a bar passing the target shows indistinguishable displayed images. Therefore, we report the period of the mask as the minimal time between identical image appearances on the screen.

Fig. 2 depicts the dependence of the perceptual state on the phase of the mask for two observers. Clearly, the disappearance report (the black lines) lacks a structure for short periods (1 sec) of mask rotation, but it was phase locked for longer periods (4 sec). The results for all observers are shown in the Supplementary Materials. For the longer rotation period (4 sec), the target was reported as visible during some phases of the stimulation cycle on practically every mask cycle, whereas during other phases, visibility reports were recorded on only 65–80 % of the cycles. This indicates that the moving bars are effective inducers of MIB. In contrast, with the shorter mask period (1 sec), the invisibility reports were uniformly distributed during the stimulation cycle, indicating that the system does not have sufficient time for relaxation from the invisible state. The simple mathematical properties of this mask enable a systematic study of the specific mechanisms governing disappearances. Moreover, at slow rotation speeds, this mask can be used to study interactions across the boundary of awareness, since for slow presentation periods the invisibility time is highly predictable. Is it possible that the moving bars amplify the phase-dependent visibility effect present in experiments with static masks? Ruling out this possibility is experimentally a challenging task, since it is well known that disappearances in the Troxler condition are rare, and the static mask is not much different in this respect (Bonneh et al., 2014). Therefore, it would require an unreasonable number of trials to collect sufficient data for the different phases of the static mask. However, Bonneh et al. (2014) showed that perceptual disappearances with a static mask display a behavior similar to that of Troxler fading, which is very different from that of MIB. For example, increasing the target contrast reduces the

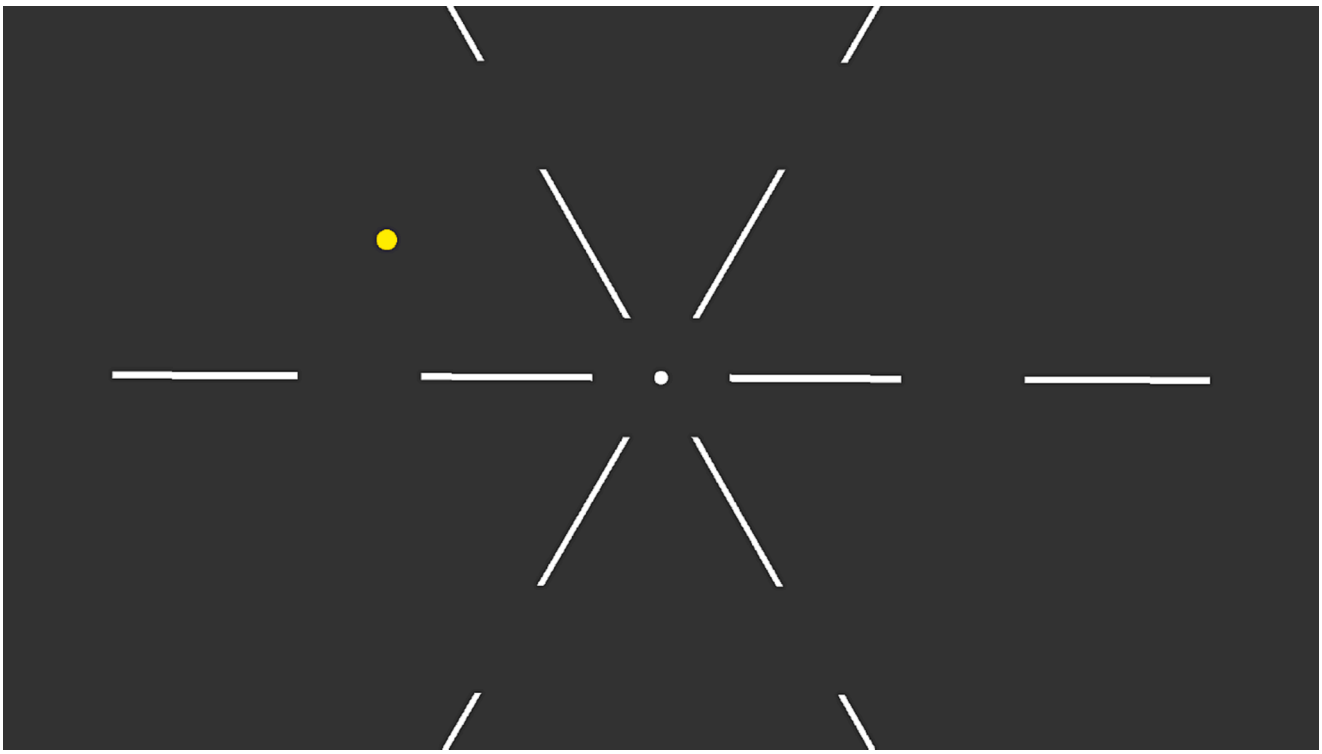

Fig. 1. An example of stimuli used in the experiments. A screenshot of a stimulus shown on a 24″ display that was viewed from 120 cm. In the experiment the mask consisted of white bars rotating around the fixation point, thus leading to periodic stimulation; the time depended on the rotation speed and the number of bars. In the static condition the stimulus was presented as depicted in the picture.

disappearance rate in static conditions (with or without a mask), while increasing the rate in MIB. Furthermore, we observed a 5-fold variation of the disappearance rate in the Troxler condition, ranging from a few events for observer O3 to a number comparable to disappearances in the moving mask conditions for observer O4 (see the distributions in Supplementary Figures S3 1–6). Observers with a high disappearance rate in the Troxler condition show reduced phase dependency in the moving mask condition. Fig. 3 illustrates the relationship between the average duration between disappearance events in the Troxler condition and the ratio between the maximum and minimum of invisibility during a stimulation period (the modulation index). Therefore, it is unlikely that MIB here results from amplification of phase dependency in the static condition.

To determine whether a refractory period is present, we examined the distribution of visible periods (Fig. 4, and Supplementary Material). One can see that all visible periods, except one in this example, are longer than 800 ms. This cannot be explained by limits on the reporting speed, since there are many invisible periods with shorter durations. Within the context of the current theory, this minimal duration is due to the system's refractory period, i.e., the system needs to recover from one invisibility epoch before transitioning to a new invisibility epoch. Thus, when the target becomes visible, it will stay visible for some minimum time. The time interval distributions for visible and invisible periods for all observers are depicted in Supplementary Fig. S3 1-6. Of the six observers, four show evidence of a refractory period when excluding a few very brief visibility events that could potentially be attributed to accidental key presses or releases during the reporting of target visibility, or rare short events influenced by the presence of noise. For observers O4 and O6, as well as observer O2, when the mask has a period of 1 s, there is a notable occurrence of numerous short visibility events. This behavior aligns with what would be expected in an excitable system with a significant noise level, as supported by the simulations presented in the Supplementary Material. However, we acknowledge that it is possible that a different mechanism may be responsible for perception in these observers.

Previous studies have explored the distribution of bistable dominance time, which refers to the duration of a single percept before switching to another percept. Some of these studies have attempted to model this distribution using a Gamma distribution (Brascamp, van Ee, Pestman, & van der Berg, 2005; Leopold & Logothetis, 1996). However, it has been reported that the data are not always well described by a Gamma distribution. Similarly, in our own experiments, we also did not obtain a good fit using the Gamma distribution. In the present experimental setup, along with the fundamental perceptual events, there is a motor execution stage, often modeled as a normally distributed random variable. Thus, we posited, as is traditionally done in modeling human reaction times, that a combination of two random variables could provide a more accurate fit to the data (Heathcote, Popiel, & Mewhort, 1991; Marmolejo-Ramos, Cousineau, Benites, & Maehara, 2015). Specifically, one variable adheres to a Gamma distribution representing the perceptual process, and the other follows a Weibull distribution. In all conditions reported here (34 conditions having more than 10 disappearance events), we obtained an excellent fit (the smallest p-value in the Kolmogorov-Smirnoff test was 0.32; see Table 1). Nevertheless, in the exploratory experiment there are some conditions, mainly the ones that employed amplitude modulation of a target that resulted in fits with very small p-values. In 231 out of 248 conditions, the distribution of the invisible periods is well described by the sum of the Gamma distributed and the Weibull distributed random variables. The literature also suggests that the Gaussian distribution describes the motor reporting (see, e.g., (Heathcote et al., 1991)). We have detailed the results of this model's excellent fit in a biorxiv preprint with the same title. However, it is important to note that random variables following a Gaussian distribution may produce arbitrarily large negative values, potentially resulting in an overall negative value for the time interval, which lacks a meaningful physical interpretation.

We have presented evidence supporting the existence of a refractory period following the invisibility state, which is clearly observed in half

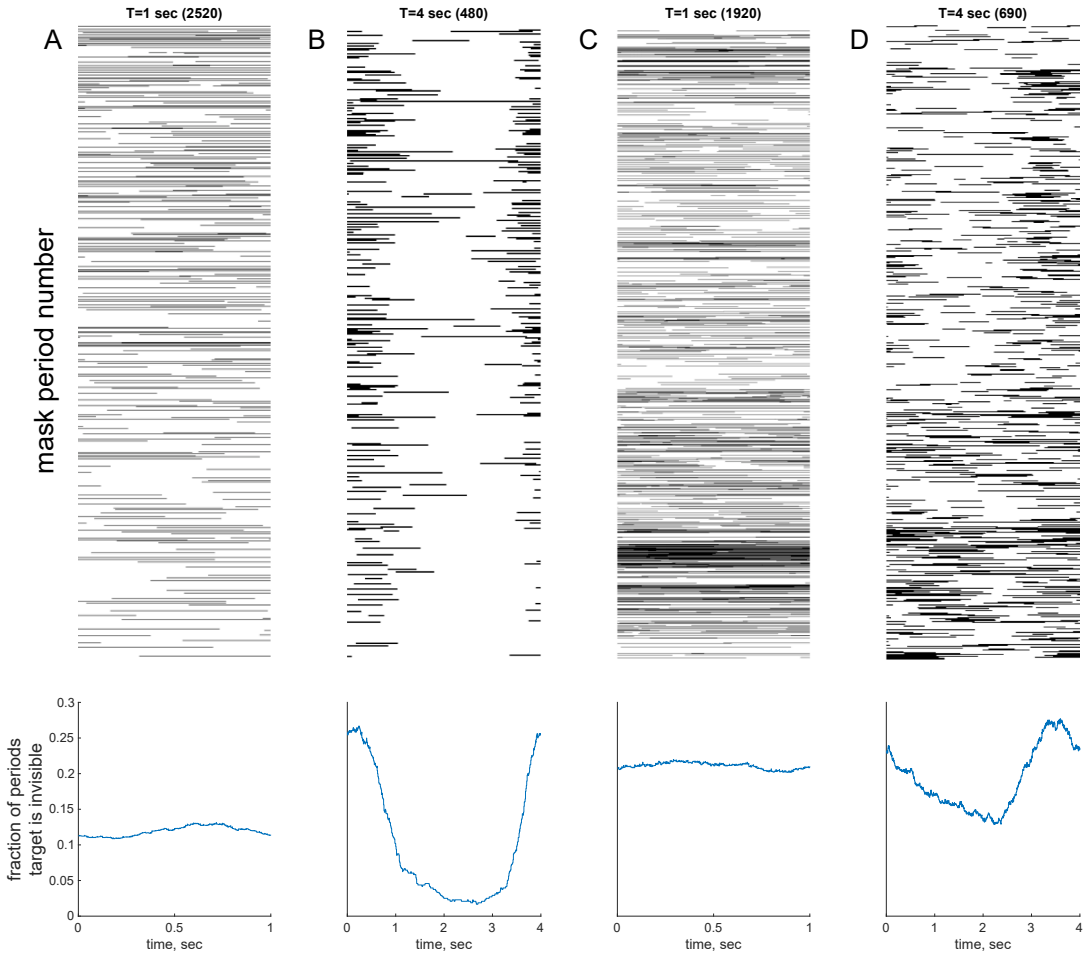

Fig. 2. Examples of the disappearance patterns from 2 participants and 2 stimulation frequencies. Top row: A raster plot of the invisibility reports. The black regions represent moments when the target was reported to be absent. Consecutive periods of mask rotation are stacked vertically. Bottom row: The disappearance rates of a target as a function of time within one stimulation cycle. (A) and (B) are the results from one human observer for mask periods of 1 sec (A) and 4 sec (B). (C) and (D) are the same as (A) and (B) obtained from another human observer. One can observe that the disappearance rate toward the end of the cycle for both observers approaches 25%, indicating the high effectiveness of the mask to induce MIB. In contrast, in the middle of the cycle for slow mask periods (B, D). there are reduced disappearance rates. For example, in (B) the target is practically always reported visible in the middle of the cycle.

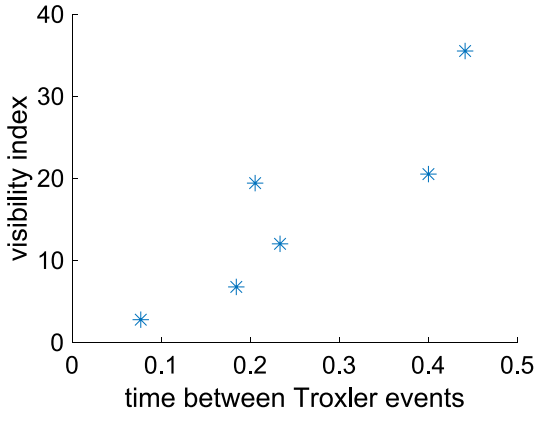

Fig. 3. Relationship between the Troxler events and the phase modulation of visibility. For each observer, we calculated the average duration between disappearances in the Troxler condition within the experimental session, and the visibility index in the MIB condition. The visibility index is defined as the maximum ratio (across all MIB conditions) between the highest and lowest fractions of periods during which the target was invisible (across different phases of stimulation). The graph illustrates a clear trend: as the frequency of Troxler events decreases, the visibility index tends to increase.

of the observers (Supplemental Fig. S3 1-6). Additionally, we have observed a delay in the dynamics before the system returns to the resting state. Next, we show the presence of noise-assisted resonance. Fig. 5 depicts the signal-to-noise ratio (SNR, see the Methods section for details) for each observer under different rotating mask periods. As one can see, for most observers there is a non-monotonic dependence of SNR on the mask frequency. One observer shows monotonic dependence, possibly indicating that the resonance is at a higher frequency. It is interesting that the optimal stimulation frequency is similar for all observers, except one, who does not show noise-assisted resonance within our experimental range. This result suggests that the dynamical properties of the mechanism underlying MIB is common to all people.

The phase-locking analysis reveals that the effectiveness of the mask is 20–30 %. For slow speeds, the disappearance events are concentrated around a specific cycle phase. Additionally, the system spends a characteristic time in the invisible state. By jointly considering these three observations, we can conclude that a bar passing near the target generally induces the target to disappear, but not always. However, when the rotation speed is fast, so that consecutive bars cross the target within a single disappearance epoch, a new disappearance event will not take place. Therefore, we would expect the statistics of the inter-disappearance events (the time between two consecutive disappearances) to correspond to the statistics of spontaneous disappearances

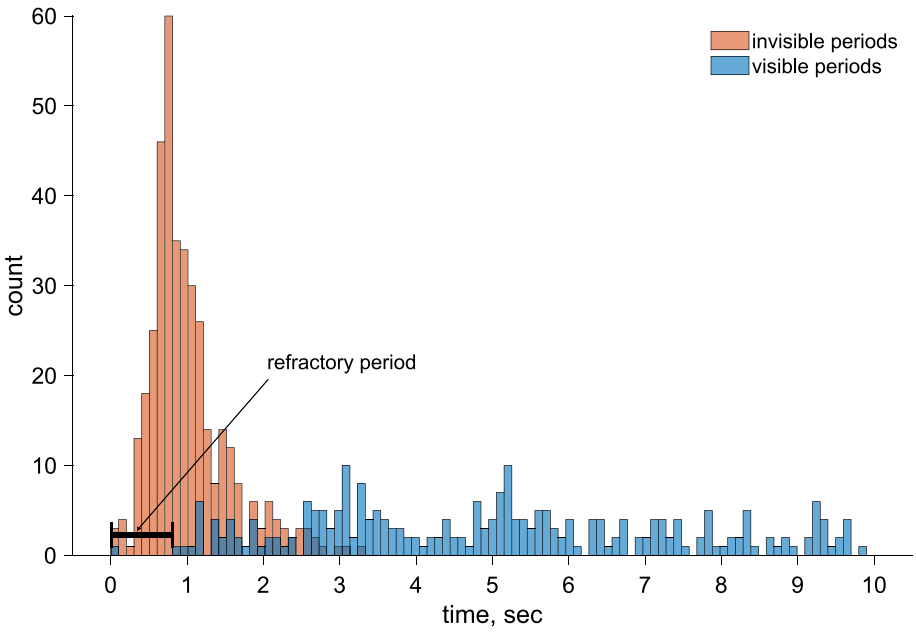

Fig. 4. Example of the distributions of the visible and invisible periods for one observer (O3) and one condition (stimulation period 2 sec). Note that visible periods can be as long as the duration of a trial, especially for the Troxler effect. These long periods are not shown on the distribution, since the time axis was cut to 10 sec to see the structure of the distribution of invisible periods.

Table 1
The distribution parameters for the disappearance times. The distributions were assumed to be the sum of two random variables, one Weibull distributed and one gamma distributed. p represents the p-value of the Kolmogorov-Smirnoff goodness of fit. All six observers are shown (3 rows × 2 columns). The condition where there are fewer than 10 disappearance events was not fitted. The highlighted columns show the constant delay before the target reappears, representing a long excursion time (~0.5 sec) in an excitable system until it returns to a stable state. One can see that these times are relatively consistent for the same observer in all experimental conditions, probably indicating prototypical dynamics. The symbol σ probably indicates the jitter in the response. The parameters of the gamma distribution are more variable, even within the same observer, possibly indicating the differential effect of the mask. For instance, one can see that the κ values are more consistent in conditions with a moving mask than in the Troxler or static mask conditions (see the condition details in the Methods section).

	p	Gamma		Weibull		p	Gamma		Weibull	
		a	b	a	b		a	b	a	b
	O1					O2				
Troxler	0.98	0.23	0.49	1.04	2.62	0.94	1.1	0.44	0.23	2.15
Static mask	0.98	1.13	0.35	0.67	3.4	1	1.24	0.32	0.17	2.68
1 sec	0.89	0.75	1.15	1.4	4.75	0.38	0.11	0.86	1.1	1.2
2 sec	0.86	0.67	0.63	1.82	2.44	0.78	1.27	0.77	0.17	2.27
4 sec	0.92	0.31	1.09	1.36	4.47	0.97	0.44	0.88	0.79	1.37
8 sec	0.98	0.62	0.89	1.12	4.75	0.83	1.12	0.41	0.64	1.04
	O3					O4				
Troxler						0.89	2	0.19	0.25	1.81
Static mask						0.95	0.76	0.34	0.56	2.22
1 sec	0.92	0.82	0.58	0.78	3.53	0.86	0.51	0.77	0.67	2.08
2 sec	0.49	1.64	0.32	0.5	2.52	0.5	1.61	0.29	0.58	2.17
4 sec	1	0.35	0.8	0.87	3	0.78	0.61	0.57	0.69	2.67
8 sec	1	0.33	0.83	0.83	3.35	0.92	1.2	0.46	0.64	2.79
	O5					O6				
Troxler	0.9	2.02	0.14	0.82	4.36	0.92	0.85	0.25	0.54	4.3
Static mask	0.91	0.27	0.2	1.1	4.49	0.97	0.82	0.02	0.52	4.9
1 sec	0.91	0.44	0.85	0.97	4.16	0.95	1.8	0.31	0.41	2.42
2 sec	0.55	0.45	0.41	0.97	4.73	0.32	1.11	0.32	0.6	2.4
4 sec	0.68	0.16	1.07	1.11	6.04	0.97	0.57	0.52	0.61	3.61
8 sec	0.92	0.13	0.74	1.31	3.87	0.93	0.3	0.59	0.69	5.22

under the limit of high rotation speed. If the rotation speed is too slow, there will be longer periods of visibility (resting states) between the induced invisible events, allowing for infrequent spontaneous events of disappearance (as in the Troxler effect) when the mask is in a favorable phase. In both cases, the distribution of the inter-disappearance times would be smeared across many timescales and would weakly depend on the stimulation frequency. For intermediate rotation speeds, where the rotation period approaches the characteristic timescale of the system, upon a state switch triggered by a favorable stimulus event, the intrinsic dynamics bring the system to a resting state, and thus to a response that is time locked to a specific phase and frequency. Since the mask does not induce a disappearance in every period, one would expect the inter-disappearance times to be predominantly multiples of the rotation period.

Fig 6 (top row) shows the inter-disappearance times for one observer. One can see that for mask periods (T) of 2, 4, and 8 s, there are peaks in

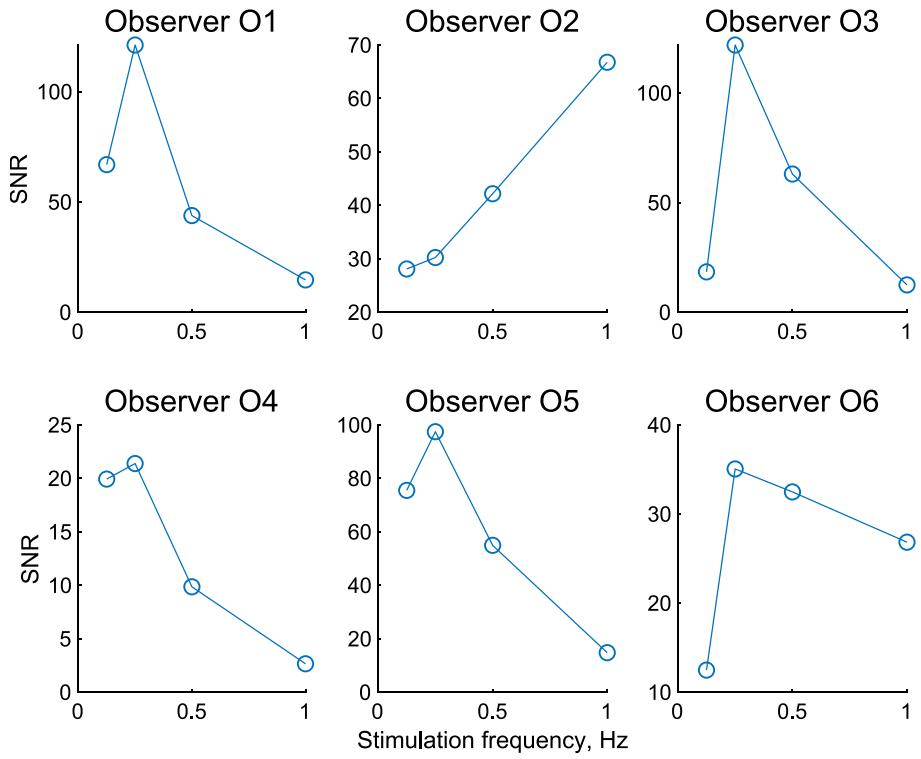

Fig. 5. Dependence of the signal-to-noise ratio (SNR) on the stimulation frequency. Each plot shows the SNR for a single observer for different mask periods (see details in the Methods section).

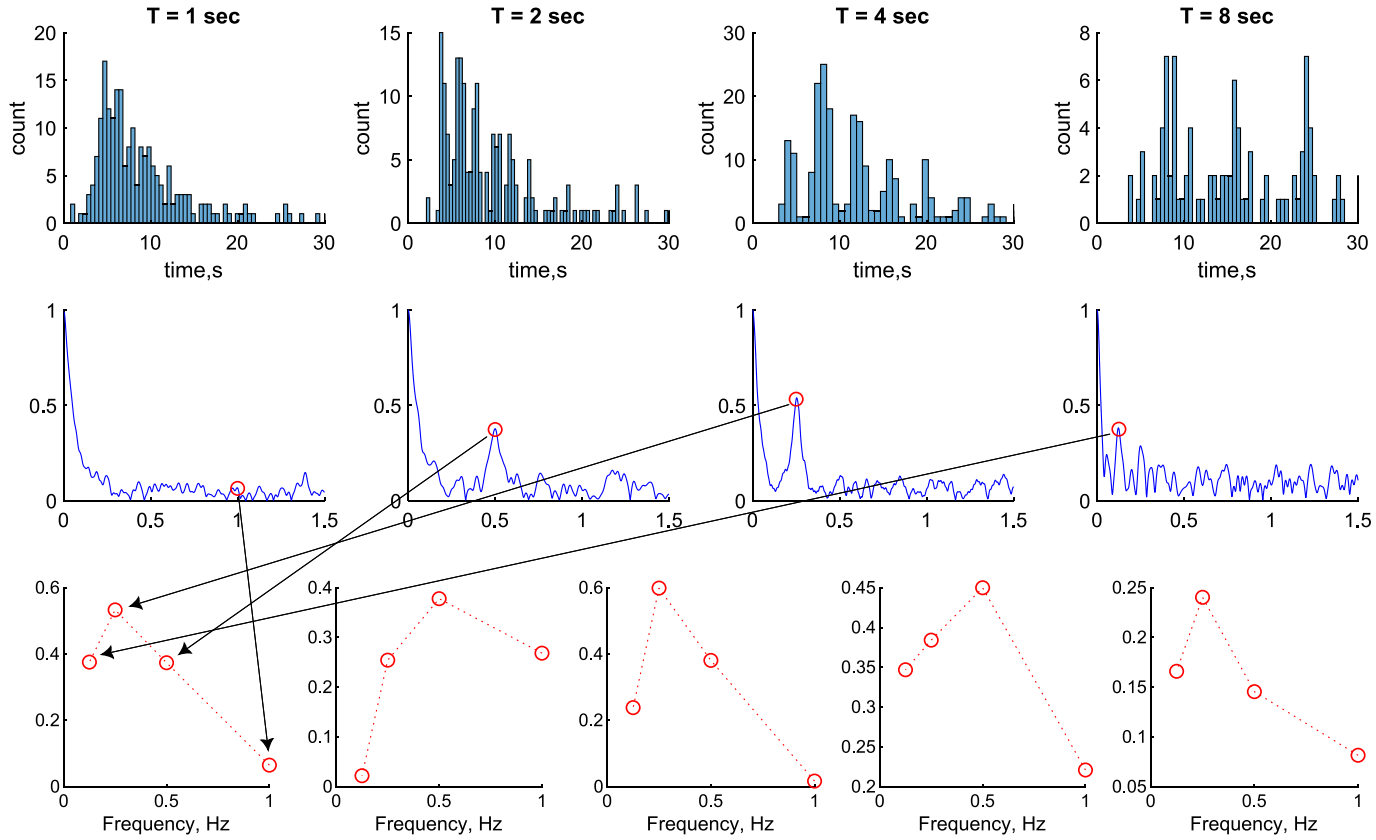

Fig. 6. Inter-disappearance times. Top row: Histograms of the inter-disappearance times for one observer during different mask periods (indicated in the subplot titles). Middle row: Amplitude for empirical characteristic functions of the distributions shown in the top row. Bottom row: Amplitudes from each characteristic function at the frequency corresponding to the frequency of the mask are shown. Each plot corresponds to the experiments performed by a single observer; the left one matches the data depicted in the top and middle rows.

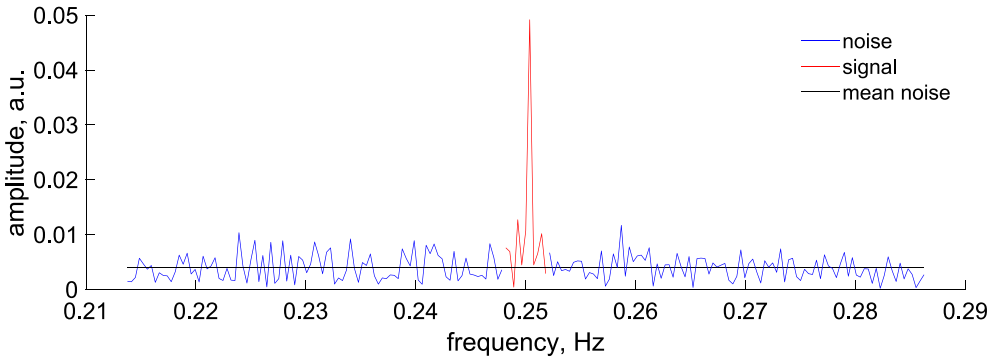

Fig. 7. Signal-to-Noise analysis. An example of an amplitude of a Fast Fourier Transform of a temporal signal that consisted of "1″ (target visible) and "0" (target invisible) sampled at 1 ms time steps for observer O5, and a 4 sec stimulation period. The Signal-to-Noise ratio was computed as the ratio between mean amplitudes of signal bins (expected stimulation frequency ± 5 bins, denoted in red) and noise bins (expected frequency ± 100 bins, excluding signal bins, denoted by a blue curve). Mean noise value is denoted by a black line.

the distributions of the inter-disappearance times corresponding to times nT, where n is an integer number, i.e., it frequently requires several mask periods before the target disappears. One can also observe that near the resonance frequency (T = 4sec, Fig. 5), the second and third times that the bar passes the target (peaks at 8 and 12 sec) are more successful in inducing disappearance than the first time is. This is expected if the rotation period is slightly faster than the characteristic timescale of the system. Here, when the system returns to a resting state, the mask has already passed the most favorable phase for switching (see Fig. 2).

Another way to see the periodicity of the function is to take its Fourier transform. A single peaked amplitude spectrum will indicate a single dominant frequency. The characteristic function (Billingsley, 1995) of the distribution is practically the Fourier transform of its probability density function (pdf). Since the pdf shape is not known, one can compute an empirical characteristic function (Cramér, 1946), and if the pdf is dominated by a periodic component, then a peak in the absolute value of the empirical characteristic function is expected. The middle row in Fig. 6 shows the absolute value of the empirical characteristic function for samples whose histograms are shown in the top row. The peaks at the stimulation frequencies are clearly seen for mask periods of 2, 4, and 8 s (red circles) – confirming that the disappearance events are predominantly spaced by the integer number of periods (nT), with many different values for the integer n. Interestingly, the amplitude of the mode corresponding to the stimulation frequency has a non-monotonic behavior (Fig. 6, bottom row for all observers). For example, for the observer shown in the top and middle rows, the peak amplitude for T = 4 sec is larger than for T = 2 sec or T = 8 sec.

The distributions and empirical characteristic functions for all observers are presented in the Supplementary Materials. The data for one observer (O4, examples of raster plots are shown in Fig. 2C,D) show no peak in the characteristic functions for any stimulation frequency. These results indicate the domination of noise in the behavior but may also reflect the low efficiency of bars as inducers for this observer. One of the indications for the former case is the similarity of the inter-disappearance distributions between moving bars, static bars, and Troxler conditions (Supplementary Figures Fig. S2 1-6).

4. Discussion

The series of experiments performed in this work indicate that rotating bars are effective inducers of target disappearance in MIB. Moreover, the effect is phase locked to the mask for long periods (Fig. 2). We observed a refractory period for most observers (Figs. 4, S3 1-6). For two observers (O4 and O6), phase locking was less pronounced (Figure S.1. 4, Figure S.1. 6), suggesting inefficient stimulation. Signal-to-noise analysis of the temporal sequences of responses showed resonance at frequencies at around 0.25 Hz, corresponding to a mask period of 4 sec (Fig. 5). In analyzing the empirical characteristic functions, we observed peaks at frequencies corresponding to integer multiples of the mask periods (Fig. 6). In other words, several mask periods are frequently required to induce a disappearance, indicating that moving bars are weak disappearance inducers and that the amount of intrinsic noise is relatively small. Additionally, in all experiments the distribution of invisibility times is well modeled by the sum of two random variables distributed according to the Gamma and Weibull distributions. The Gamma distribution was frequently considered for describing switching dynamics in bistable systems. We added the Weibull distribution to absorb temporal jitter when executing a motor command to either press or release a keyboard key and the mean time required for a long excursion of the system until it returns to a resting state. In the Supplementary Materials we present the simulation of an excitable system that shows similar behavior. Therefore, we concluded that the mechanisms responsible for MIB may operate in the regime of an excitable system.

Our data point to local effects of the mask on the target, since in the slow conditions there is an increased rate of disappearance at a specific phase of mask rotation. Uncovering the mechanisms underlying these effects is not easy, since there are observer-dependent relatively long delays in the observers' reports. For example, (Donner, Sagi, Bonneh, & Heeger, 2008) replayed simulated MIB visibility sequences to observers, with the target physically erased at stimulation times when invisibility was previously reported in the presence of continuous stimulation. Observers' reaction times to the physical disappearance ranged between 500 and 800 msec. This delay needs to be added with the time required for perceptual visibility-invisibility transition, assumed to be around ~400 ms (Meital-Kfir & Sagi, 2018). Therefore, the expected delay is about 1 sec, which is 1/8 of a cycle in our slowest condition with undefined variability of these delays. However, by introspection, the target disappears when the bars are near the target. Given the results obtained in (May, Tsiappoutas, & Flanagan, 2003) pointing out that an abrupt contrast decrement leads to target disappearance, and that known masking effects, such as metacontrast masking (Alpert, 1953) possibly affect the target, it suggests that the moving, but not the static mask induces local abrupt changes in perceived contrast by masking effects that consequently trigger target disappearance.

One of the models used in the past to study bistable perception describes perceptual switches by the random motion of a "particle" in a double-well potential. In this model, the decision variable corresponds to a one-dimensional coordinate of a "particle" inside a potential with two local minima (two wells), separated by a barrier. In the absence of noise, the "particle" "falls" to the position of the nearest local minimum and stays there indefinitely. In the presence of noise, however, the "particle" has a chance to gain enough energy to overcome the barrier

and move to another well, and it will subsequently fall to another local minimum. Translating this to perception, it is usually assumed that when a "particle" is close to one minimum, one image is perceived, and when the "particle" is close to another minimum, another image is perceived. Kim et al., 2006, introduced this one-dimensional model to study binocular rivalry. Nevertheless, it is hard to extend this formalism to describe the quasi-stable perception in MIB or the Troxler effect (Troxler, 1804). Here we suggest that the theory of excitable systems is a suitable framework for describing MIB. Although the practical implementation in a biological network can be quite complicated, the simplest formal model describing excitable systems is the FitzHugh-Nagumo model (FitzHugh, 1961; Nagumo, Arimoto, & Yoshizawa, 1962; Sherwood, 2014). It assumes that the neuronal dynamics can be effectively described by two one-dimensional variables with substantially different timescales of evolution. The variable having fast dynamics can be interpreted as a decision variable in the double-well model. In contrast, the variable with slow dynamics is assumed to represent processes such as adaptation (Caetta, Gorea, & Bonneh, 2007; Gorea & Caetta, 2009), filling-in (Hsu et al., 2006), motion streaks (Wallis & Arnold, 2009), depth ordering, and surface completion (Graf, Adams, & Lages, 2002). Within this proposal, there is a perceptual criterion on the "fast" decision variable, so that a target is reported invisible when this criterion is crossed but is reported visible when the criterion crossing yields a decision that is in the opposite direction.

By changing parameters in the same noisy FitzHugh-Nagumo model, one can describe other bistable phenomena such as binocular rivalry. This description can be general enough to describe all stable, bistable, and quasi-stable perceptual phenomena. Furthermore, stable fixed points of dynamical systems, forming attractors, constitute the basis for the memory models in the attractor neural networks (ANN). In these networks, the memory items are assumed to be recalled, or perceived when the pattern of network activity is close enough to one of the stored patterns of activity (memory). Technically, when the overlap (correlation) between the activity and the stored memory exceeds some threshold value, the model is assumed to recall this stored memory. In other words, the overlap measure can be considered a decision variable. A memory item is then recalled (perceived as this specific item) when the dynamics of the network activity are near the memorized pattern (the fixed point of the dynamics), for example, the resting state in MIB or stable percepts in bistable phenomena. Thus, a possible interpretation of MIB follows, so that both the static target and the moving mask are each consistent with some attractor states in the brain corresponding to their generated percepts, whereas both together are inconsistent with any attractor. Here, the mask plays the role of a force driving the network state away from an otherwise stable attractor that corresponds to the static target perception. It appears that there are no other stable attractors near the target (meaning that there is no stable illusory percept), and that the network dynamics relax (after a long excursion) into the stable state, yielding a visible target. During state transition, there is no stored pattern along the path of the dynamics that can be interpreted as target presence; therefore, the target stays perceptually invisible.

By considering the dynamics of the nonlinear systems near the bifurcation point in the context of the Attractor Neural Network model of memory, we speculate that the conscious state consists of activating a specific attractor associated with a specific memory. Once the network is driven away from the attractor, the brain becomes unaware of the physical stimulus until the network dynamics return to the memory attractor associated with any stimulus. Despite that the brain is unaware of the physical stimulus, the stimulus drives the dynamics of the network, allowing an interaction across the boundary of awareness (Meital-Kfir & Sagi, 2018; Meital-Kfir, Bonneh, & Sagi, 2016). As in the initial stage of testing these speculations, we established here that MIB operates in a regime similar to that of an excitable system.

5. Declaration of Generative AI and AI-assisted technologies in the writing process

During the preparation of this work the author(s) used chatGPT to improve the grammar and text consistency. After using this tool/service, the authors reviewed and edited the content as needed and take full responsibility for the content of the publication.

CRediT authorship contribution statement

Mikhail Katkov: Conceptualization, Formal analysis, Investigation, Writing – original draft, Writing – review & editing. **Alexander Cooperman:** Conceptualization, Investigation, Data curation. **Noya Meital-Kfir:** Data curation, Writing – review & editing. **Dov Sagi:** Investigation, Project administration, Resources, Writing – review & editing.

Declaration of competing interest

The authors declare that they have no known competing financial interests or personal relationships that could have appeared to influence the work reported in this paper.

Data availability

Data will be made available on request.

Acknowledgment

This work was supported by the Basic Research Foundation administered by the Israel Academy of Sciences and Humanities (grant No. 6501560).

.

Appendix A. Supplementary data

Supplementary data to this article can be found online at https://doi.org/10.1016/j.visres.2024.108363.

References

Alpert, M. (1953). Metacontrast. *Journal of the Optical Society of America, 43*(8). https://doi.org/10.1364/josa.43.000648

Billingsley, P. (1995). *Probability and Measure* (3rd ed.). Wiley-Interscience Publication.

Bonneh, Y. S., Cooperman, A., & Sagi, D. (2001). Motion-induced blindness in normal observers. *Nature, 411*(6839), 798–801. https://doi.org/10.1038/35081073

Bonneh, Y. S., Donner, T. H., Cooperman, A., Heeger, D. J., & Sagi, D. (2014). Motion-Induced Blindness and Troxler Fading: Common and Different Mechanisms. *PLoS One1, 9*(3), e92894.

Brascamp, J. W., van Ee, R., Pestman, W. R., & van der Berg, A. V. (2005). Distributions of alternation rates in various forms of bistable perception. *Journal of Vision, 5*(4). https://doi.org/10.1167/5.4.1

Braun, J., & Mattia, M. (2010). Attractors and noise: Twin drivers of decisions and multistability. *NeuroImage*. https://doi.org/10.1016/j.neuroimage.2009.12.126

Caetta, F., Gorea, A., & Bonneh, Y. (2007). Sensory and decisional factors in motion-induced blindness. *Journal of Vision, 7*(7). https://doi.org/10.1167/7.7.4

Cao, R., Pastukhov, A., Aleshin, S., Mattia, M., & Braun, J. (2021). Binocular rivalry reveals an out-of-equilibrium neural dynamics suited for decision-making. *eLife, 10*. https://doi.org/10.7554/ELIFE.61581

Carter, O. L., & Pettigrew, J. D. (2003). A Common Oscillator for Perceptual Rivalries? *Perception, 32*(3), 295–305. https://doi.org/10.1068/p3472

Cramér, H. (1946). *Mathematical Methods of Statistics (PMS-9)*. *Mathematical Methods of Statistics (PMS-9)*. https://doi.org/10.1515/9781400883868.

Devyatko, D., Appelbaum, L. G., & Mitroff, S. R. (2017). A Common Mechanism for Perceptual Reversals in Motion-Induced Blindness, the Troxler Effect, and Perceptual Filling-In. *Perception, 46*(1), 50–77. https://doi.org/10.1177/0301006616672577

Donner, T. H., Sagi, D., Bonneh, Y. S., & Heeger, D. J. (2008). Opposite neural signatures of motion-induced blindness in human dorsal and ventral visual cortex. *Journal of Neuroscience, 28*(41). https://doi.org/10.1523/JNEUROSCI.2371-08.2008

FitzHugh, R. (1961). Impulses and Physiological States in Theoretical Models of Nerve Membrane. *Biophysical Journal, 1*(6). https://doi.org/10.1016/S0006-3495(61)86902-6

Gammaitoni, L., Jung, P., & Marchesoni, F. (1998). Stochastic resonance RMP p223_1.pdf. Retrieved from https://journals-aps-org.ezproxy.weizmann.ac.il/rmp/pdf/10.1103/RevModPhys.70.223.

Gorea, A., & Caetta, F. (2009). Adaptation and prolonged inhibition as a main cause of motion-induced blindness. *Journal of Vision, 9*(6), 16. https://doi.org/10.1167/9.6.16

Graf, E. W., Adams, W. J., & Lages, M. (2002). Modulating motion-induced blindness with depth ordering and surface completion. *Vision Research, 42*(25). https://doi.org/10.1016/S0042-6989(02)00390-5

Heathcote, A., Popiel, S. J., & Mewhort, D. J. (1991). Analysis of response time distributions: An example using the Stroop task. *Psychological Bulletin, 109*(2). https://doi.org/10.1037//0033-2909.109.2.340

Hsu, L.-C., Yeh, S.-L., & Kramer, P. (2006). A common mechanism for perceptual filling-in and motion-induced blindness. *Vision Research, 46*(12), 1973–1981. https://doi.org/10.1016/J.VISRES.2005.11.004

Jaworska, K., & Lages, M. (2014). Fluctuations of visual awareness: Combining motion-induced blindness with binocular rivalry. *Journal of Vision, 14*(11). https://doi.org/10.1167/14.11.11.doi

Leopold, D. A., & Logothetis, N. K. (1996). Activity changes in early visual cortex reflect monkeys' percepts during binocular rivalry. *Nature, 379*(6565). https://doi.org/10.1038/379549a0

Longtin, A., & Chialvo, D. R. (1998). Stochastic and Deterministic Resonances for Excitable Systems. *Physical Review Letters, 81*(18), 4012. https://doi.org/10.1103/PhysRevLett.81.4012

Marmolejo-Ramos, F., Cousineau, D., Benites, L., & Maehara, R. (2015). On the efficacy of procedures to normalize Ex-Gaussian distributions. *Frontiers in Psychology, 6*(JAN). https://doi.org/10.3389/fpsyg.2014.01548

May, J. G., Tsiappoutas, K. M., & Flanagan, M. B. (2003). Disappearance elicited by contrast decrements. *Perception and Psychophysics, 65*(5). https://doi.org/10.3758/BF03194812

Meital-Kfir N,Bonneh Y,Sagi D (2016) Asymmetric visual interactions across the boundary of awareness. Journal of Vision, (2016), 16(10), 4-4 doi: , 4-4 doi: 10.1167/16.10.4.

Meital-Kfir, N., & Sagi, D. (2018). Real-time visual interactions across the boundary of awareness. *Scientific Reports, 8*(1), 6442. https://doi.org/10.1038/s41598-018-24554-1

Muratov, C. B., Vanden-Eijnden, E., & Weinan, E. (2005). Self-induced stochastic resonance in excitable systems. *Physica D: Nonlinear Phenomena, 210*(3–4), 227–240. https://doi.org/10.1016/J.PHYSD.2005.07.014

Nagumo, J., Arimoto, S., & Yoshizawa, S. (1962). An Active Pulse Transmission Line Simulating Nerve Axon*. *Proceedings of the IRE, 50*(10). https://doi.org/10.1109/JRPROC.1962.288235

Sherwood, W. E. (2014). FitzHugh–Nagumo Model. In *Encyclopedia of Computational Neuroscience* (pp. 1–11). https://doi.org/10.1007/978-1-4614-7320-6_147-1.

Sparrow, J. E., LaBarre, J. A., & Merrill, B. S. (2017). Individual differences in motion-induced blindness: The effects of mask coherence and depth ordering. *Vision Research, 141*, 117–126. https://doi.org/10.1016/J.VISRES.2016.11.008

Troxler, I. P. V. (1804). Uber das Verschwinden gegebener Gegenstande innerhalb unseres Gesichtskreises. *Ophthalmologische Bibliothek, 2*(2).

Volkov, E. I., Ullner, E., Zaikin, A. A., & Kurths, J. (2003). Oscillatory amplification of stochastic resonance in excitable systems. *Physical Review E - Statistical Physics, Plasmas, Fluids, and Related Interdisciplinary Topics, 68*(2), 7. https://doi.org/10.1103/PhysRevE.68.026214

Wallis, T. S. A., & Arnold, D. H. (2009). Motion-Induced Blindness and Motion Streak Suppression. *Current Biology, 19*(4). https://doi.org/10.1016/j.cub.2008.12.053